清華大學物理系 奈米物理特論 2008/03/13 上課內容 (II)

奈米物理特論

半導體奈米結構之成長與光電特性

交通大學電子物理系　周武清 教授

大綱:

Part I:　半導體奈米結構成長---------

分子束磊晶(MBE, molecular beam epitaxy)

半導體奈米結構形貌研究---AFM

Part II:　半導體奈米結構光電特性---Photoluminescence

Part III: 半磁性半導體奈米結構之自旋磁光特性

Photoluminescence (PL)

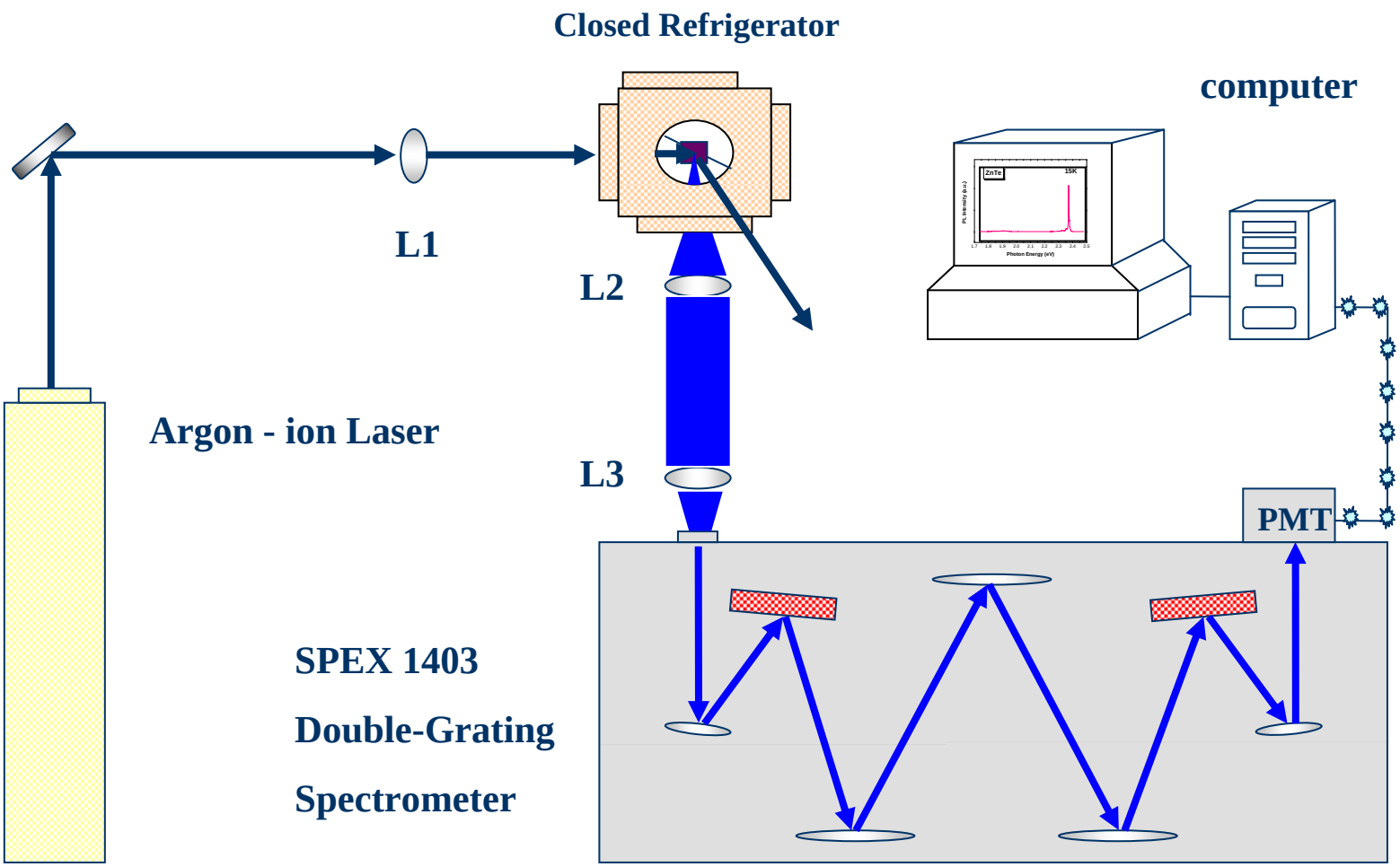

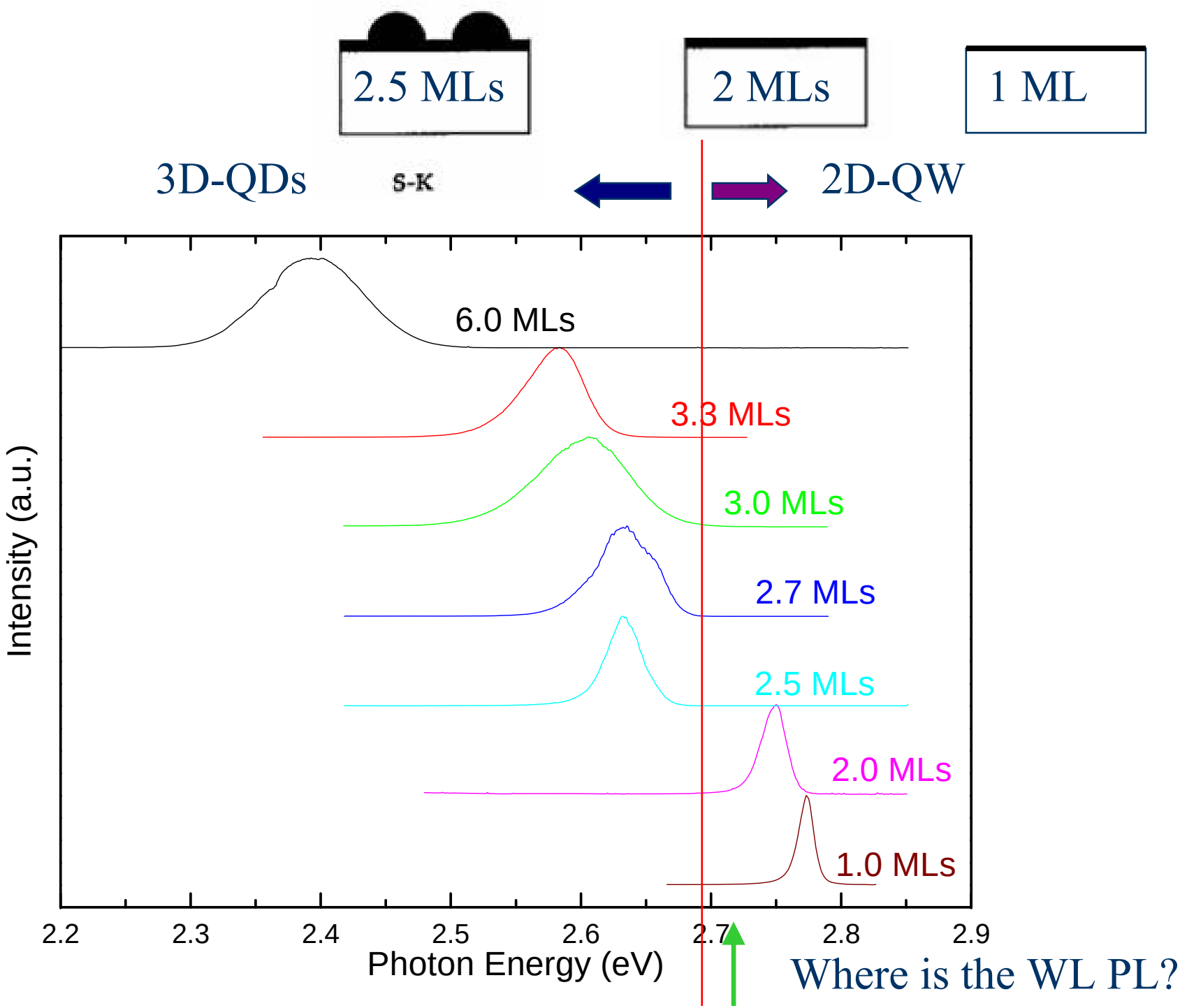
2.5 MLs
2 MLs
1 ML
3D-QDs
S-K
2D-QW
6.0 MLs
3.3 MLs
3.0 MLs
2.7 MLs
2.5 MLs
2.0 MLs
1.0 MLs
Intensity (a.u.)
2.2
2.3
2.4
2.5
2.6
2.7
2.8
2.9
Photon Energy (eV)
Where is the WL PL?

Peak position vs. CdSe coverage :

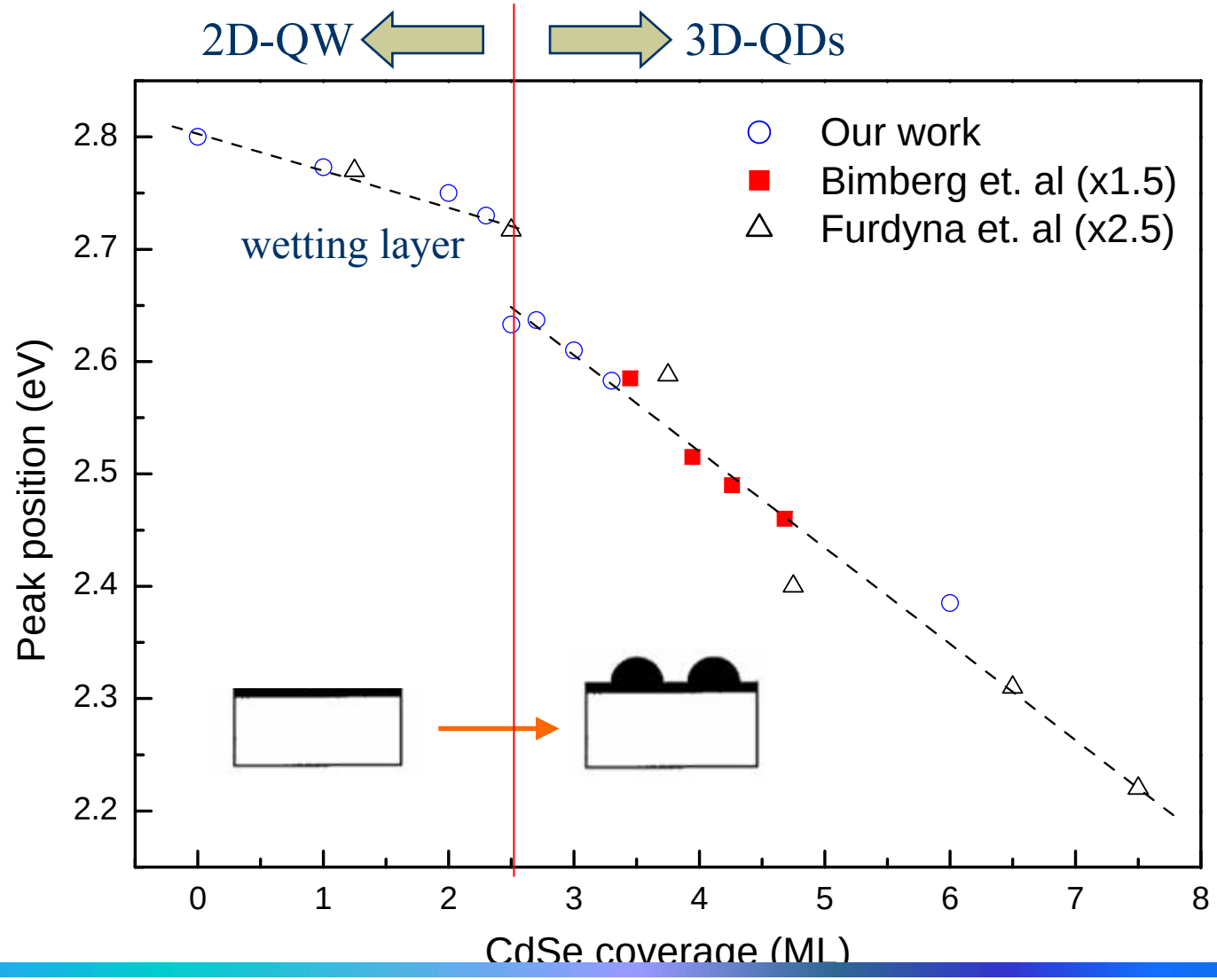

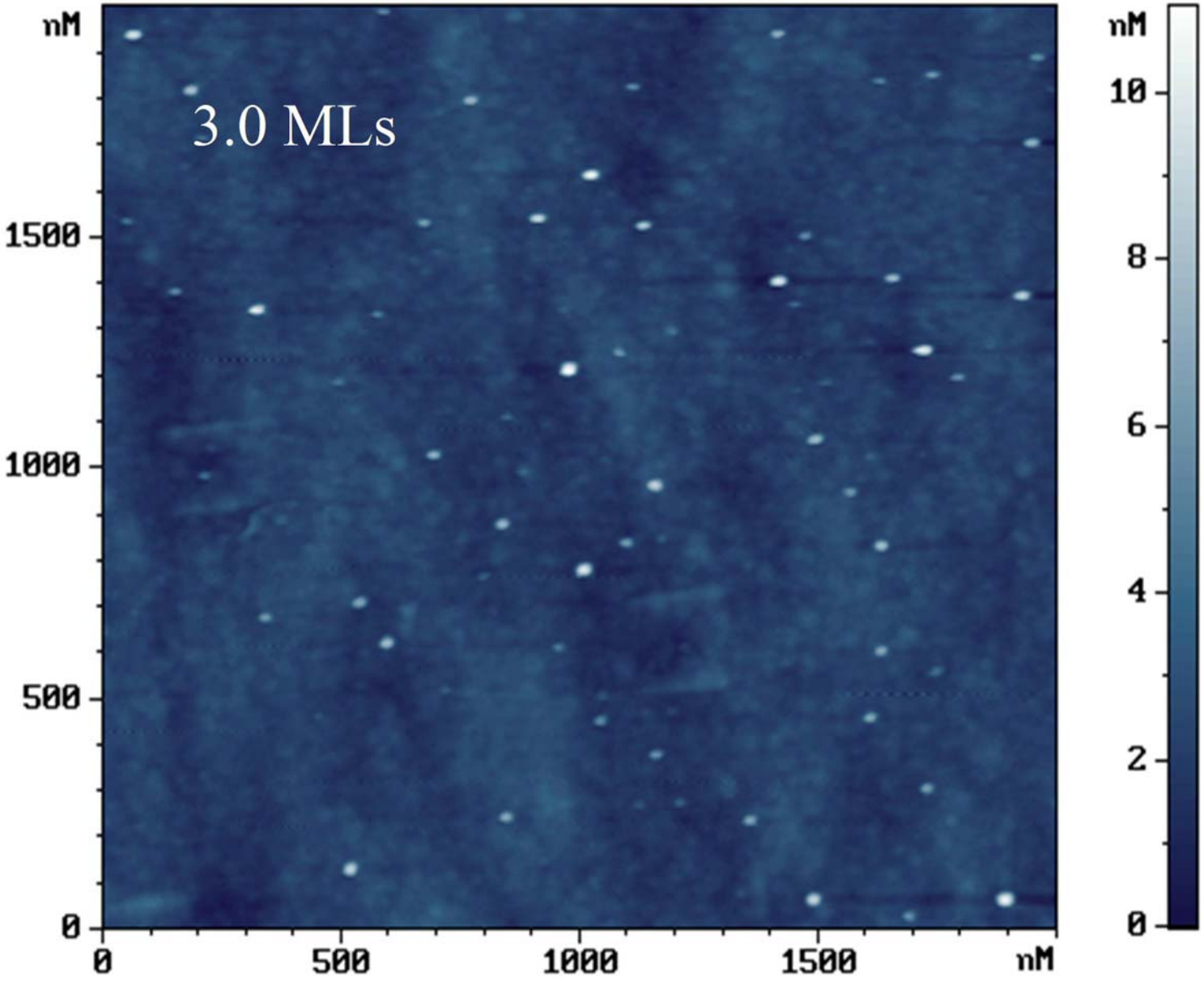

The top-view AFM image of the ZnTe QDs with coverage of 3.0 MLs.

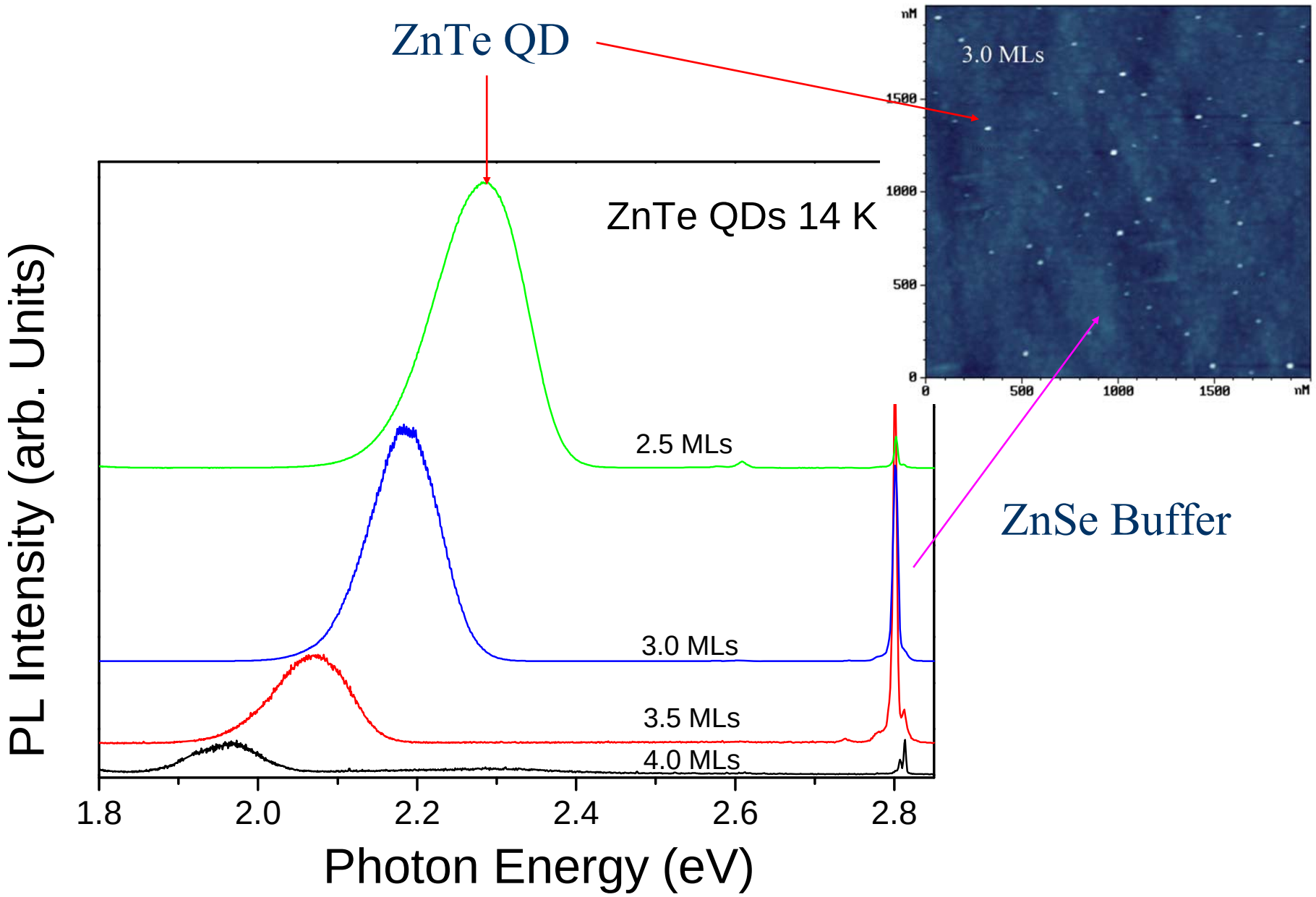

Photoluminescence spectra of the ZnTe QDs with coverage of 2.5, 3.0, 3.5, and 4.0 MLs.

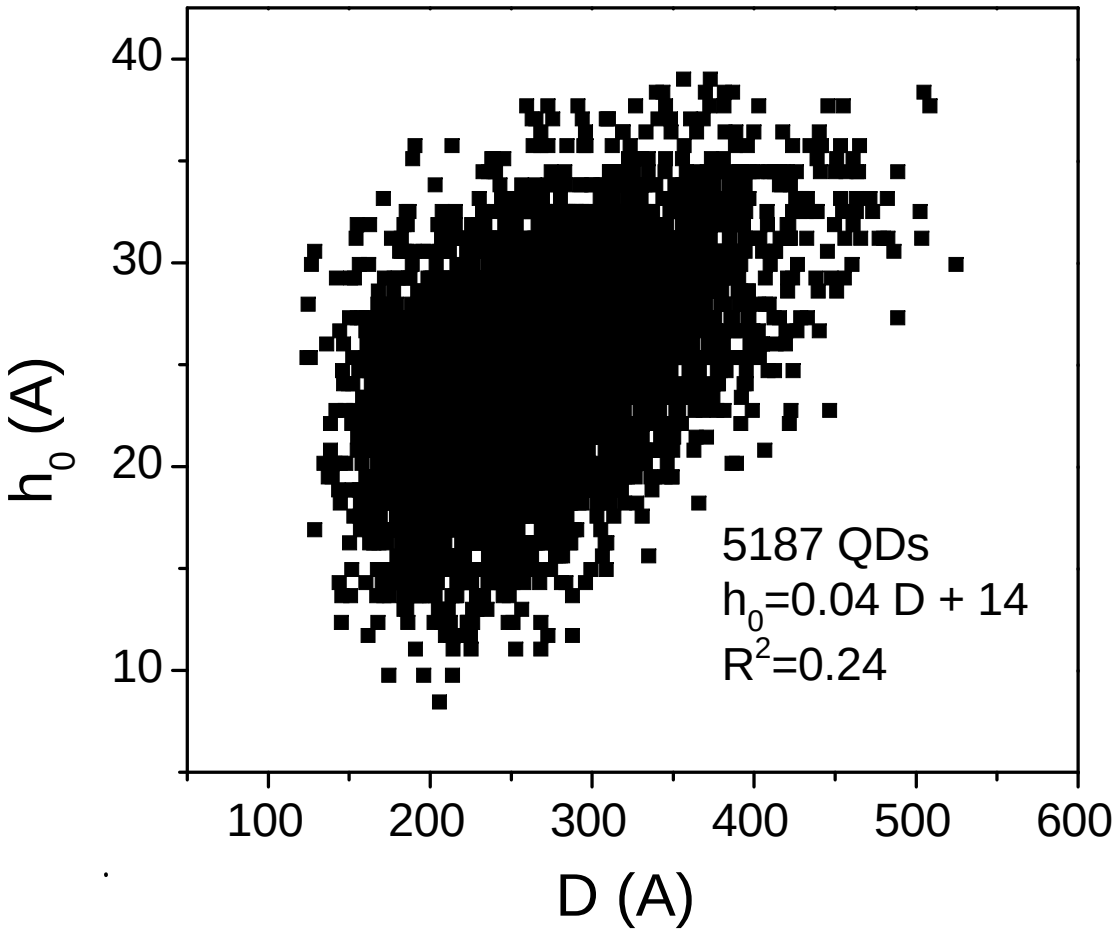

Dot size distribution: number of QDs N_{QD} versus base diameter D and height h_0 in Å measured by AFM. There are 5187 dots in an area of 3x3 μm2.

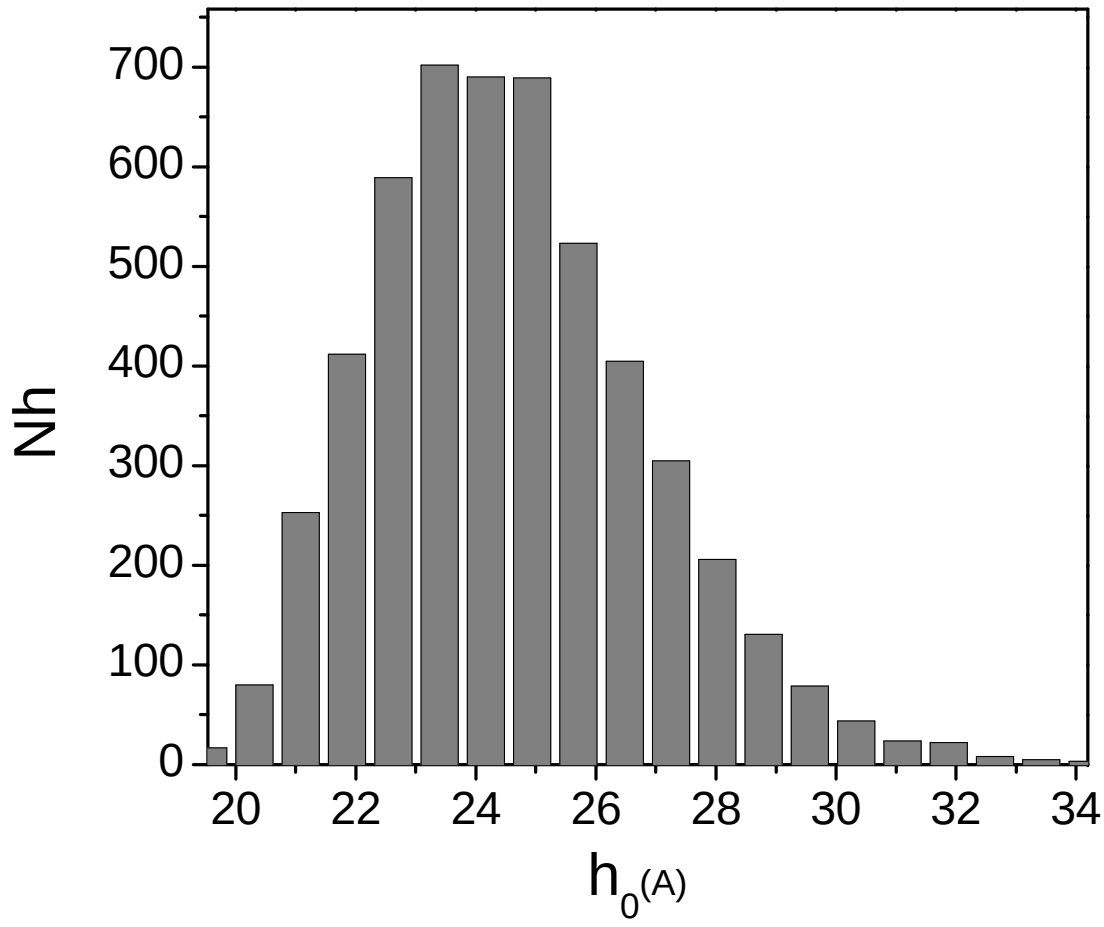

Histogram of number N_h versus h_0. N_h is a sum of the number of dots over all possible D's with the same height h_0.

Orthogonal periodic functions (OPF)

collaborator: Dr. Johnson Lee (theoretical calculations)

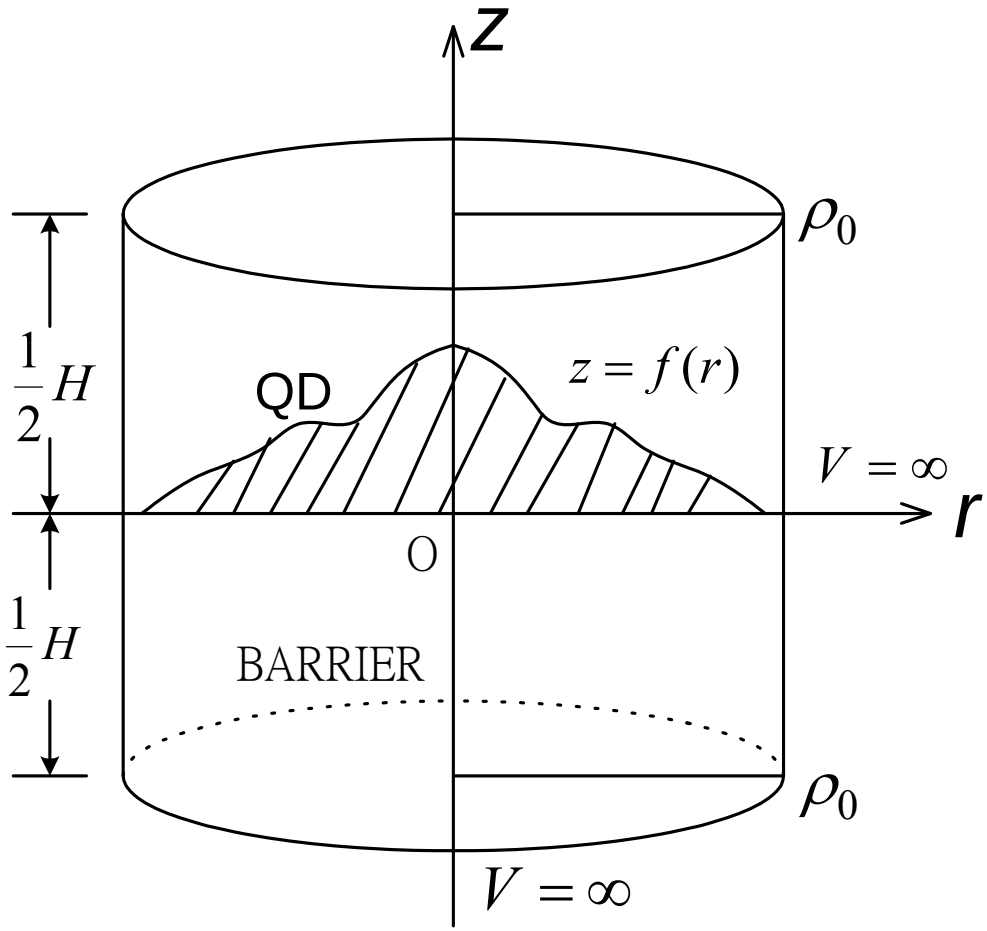

$$\psi_{nml}(r,\varphi,z) = R_{nm}(r)\, Z_l(z)\, \Phi_m(\varphi)$$

$$R_{nm}(r) = \frac{\sqrt{2}}{\rho_0 J_{m+1}(k_n \rho_0)} J_m(k_n r), \qquad 0 \le r \le \rho_0$$

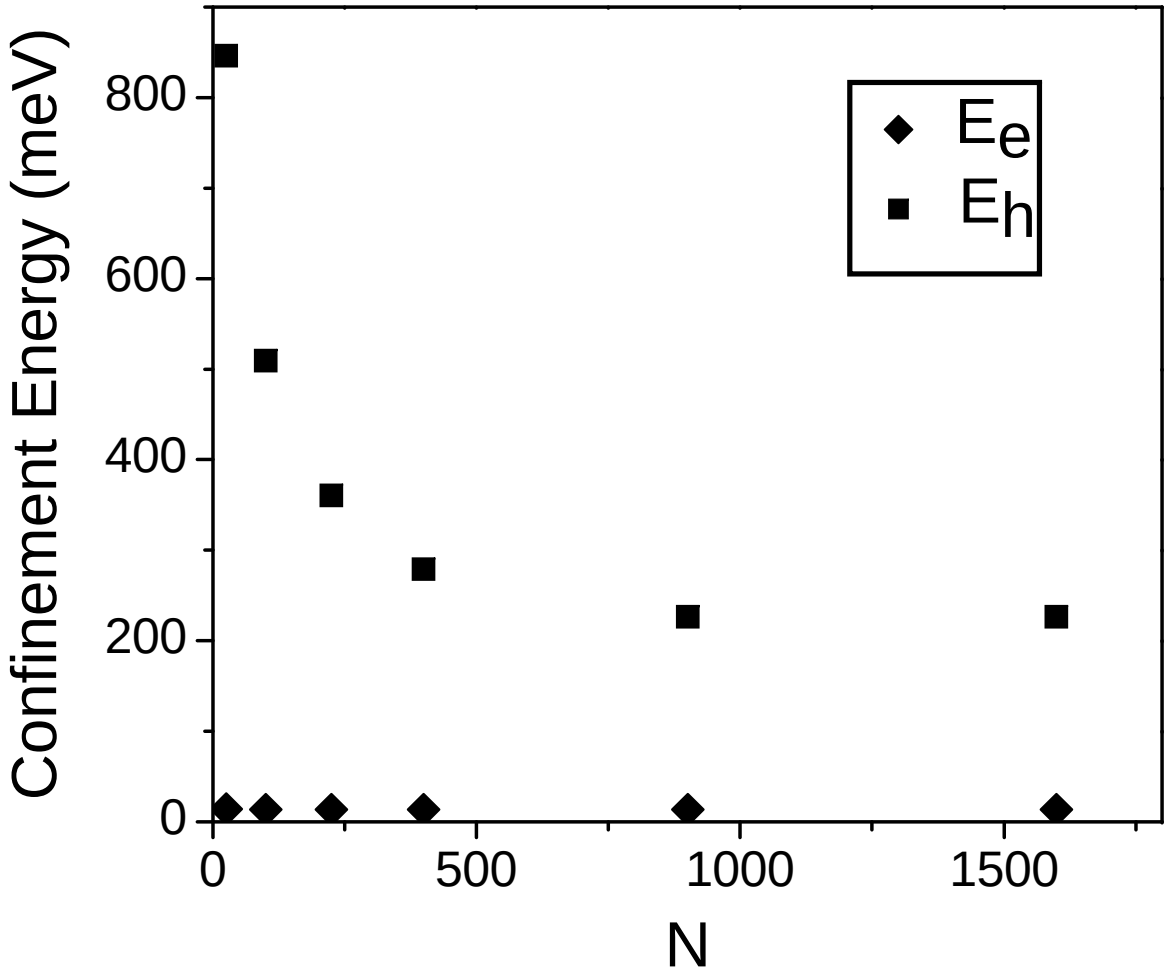

N is the matrix dimension.

For $N \geqq 900$, E_e and E_h converge.

solved a 900x900 matrix for the sub-band energies as a function of q

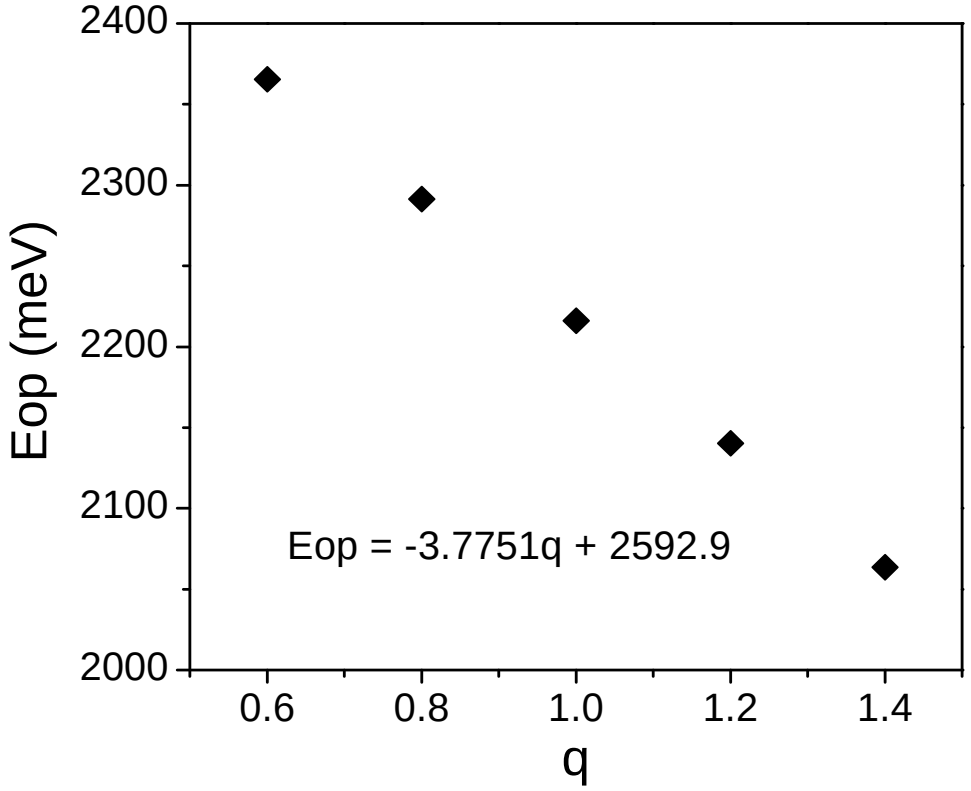

For Q=1.1, Eop=2185 meV

$\Delta E_c = q\,\Delta E_g\,(0.420eV) = 315meV \quad \Delta E_v = (1+q)E_g = 735\ meV$

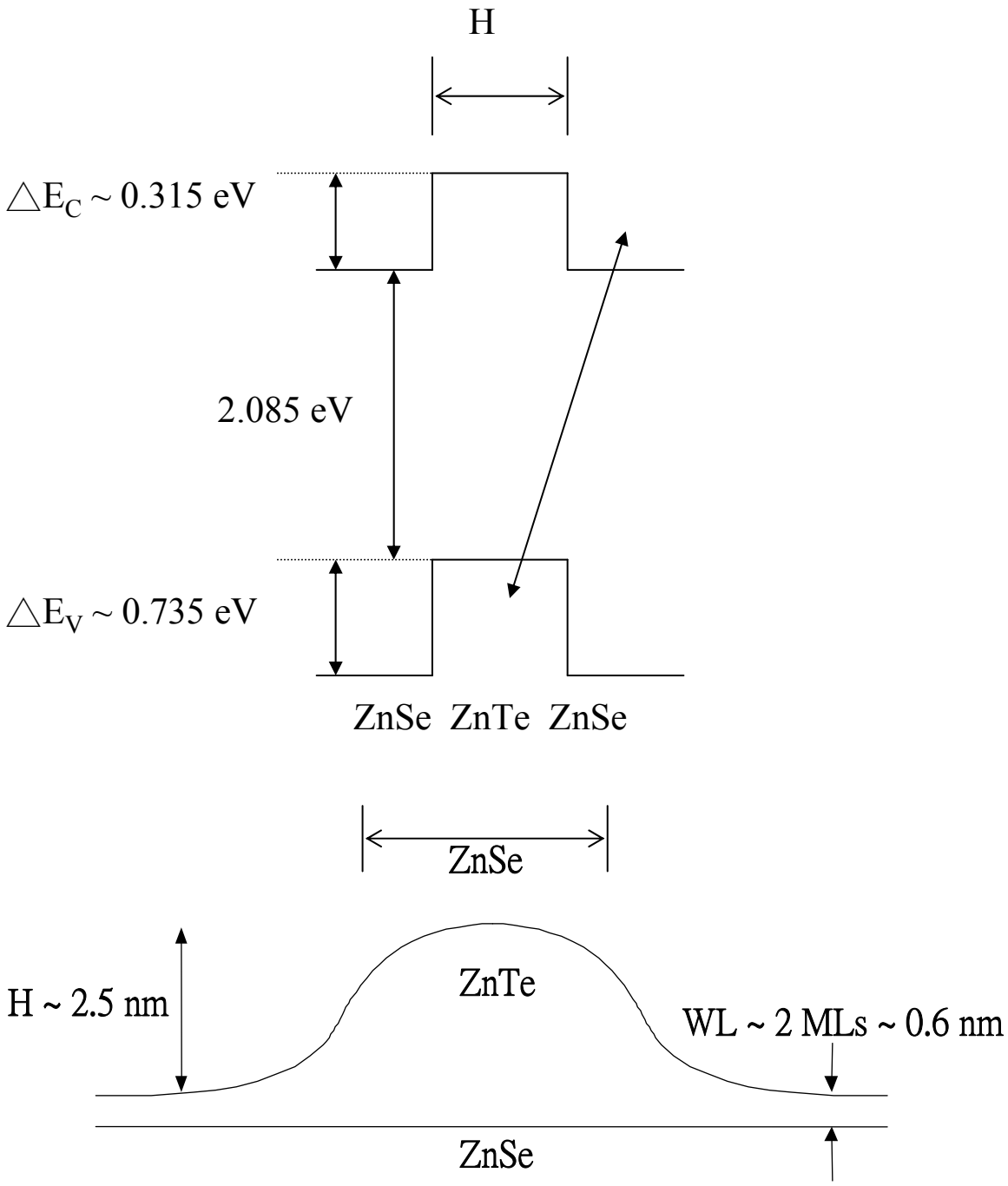
H
△E_C ~ 0.315 eV
2.085 eV
△E_V ~ 0.735 eV
ZnSe ZnTe ZnSe
ZnSe
H ~ 2.5 nm
ZnTe
WL ~ 2 MLs ~ 0.6 nm
ZnSe

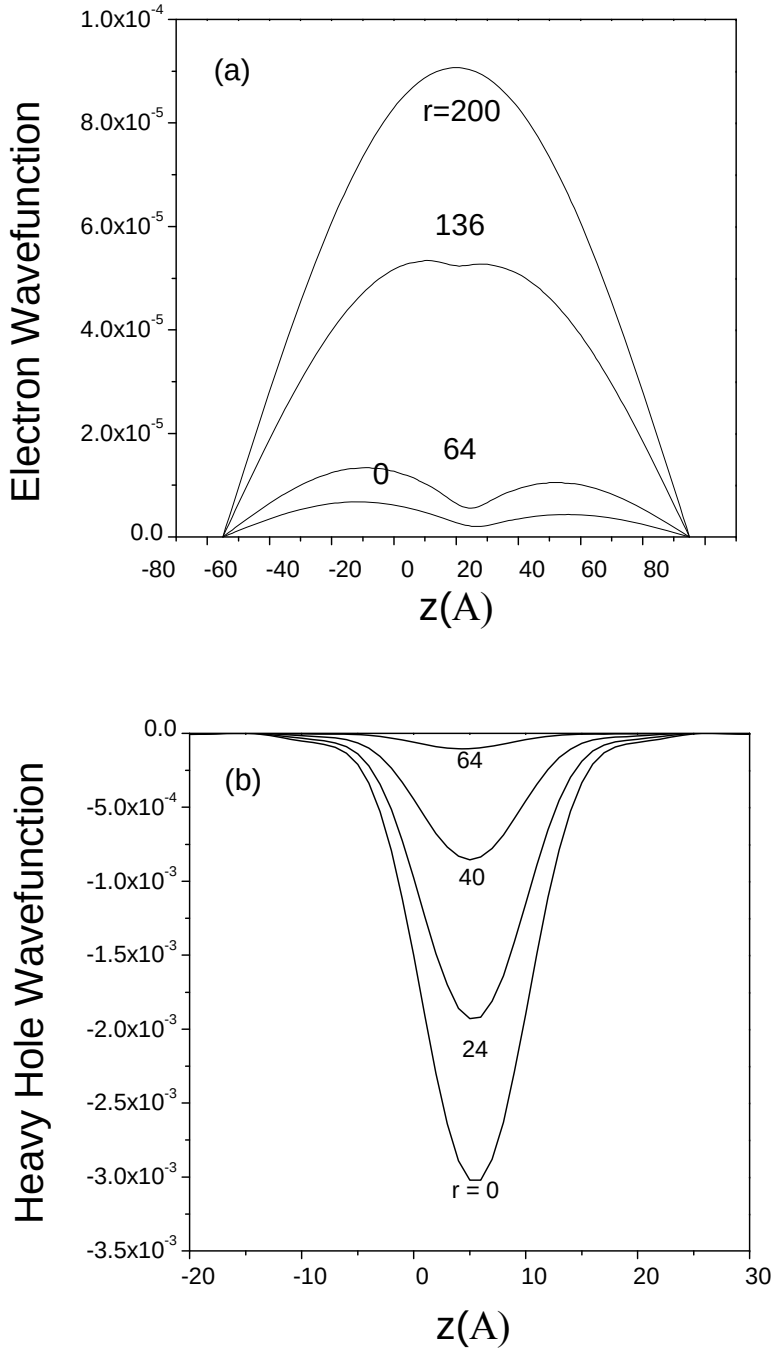
(a)
Electron Wavefunction
1.0x10-4
8.0x10-5
6.0x10-5
4.0x10-5
2.0x10-5
0.0
r=200
136
64
0
-80
-60
-40
-20
0
20
40
60
80
z(A)
(b)
Heavy Hole Wavefunction
0.0
-5.0x10-4
-1.0x10-3
-1.5x10-3
-2.0x10-3
-2.5x10-3
-3.0x10-3
-3.5x10-3
64
40
24
r = 0
-20
-10
0
10
20
30
z(A)

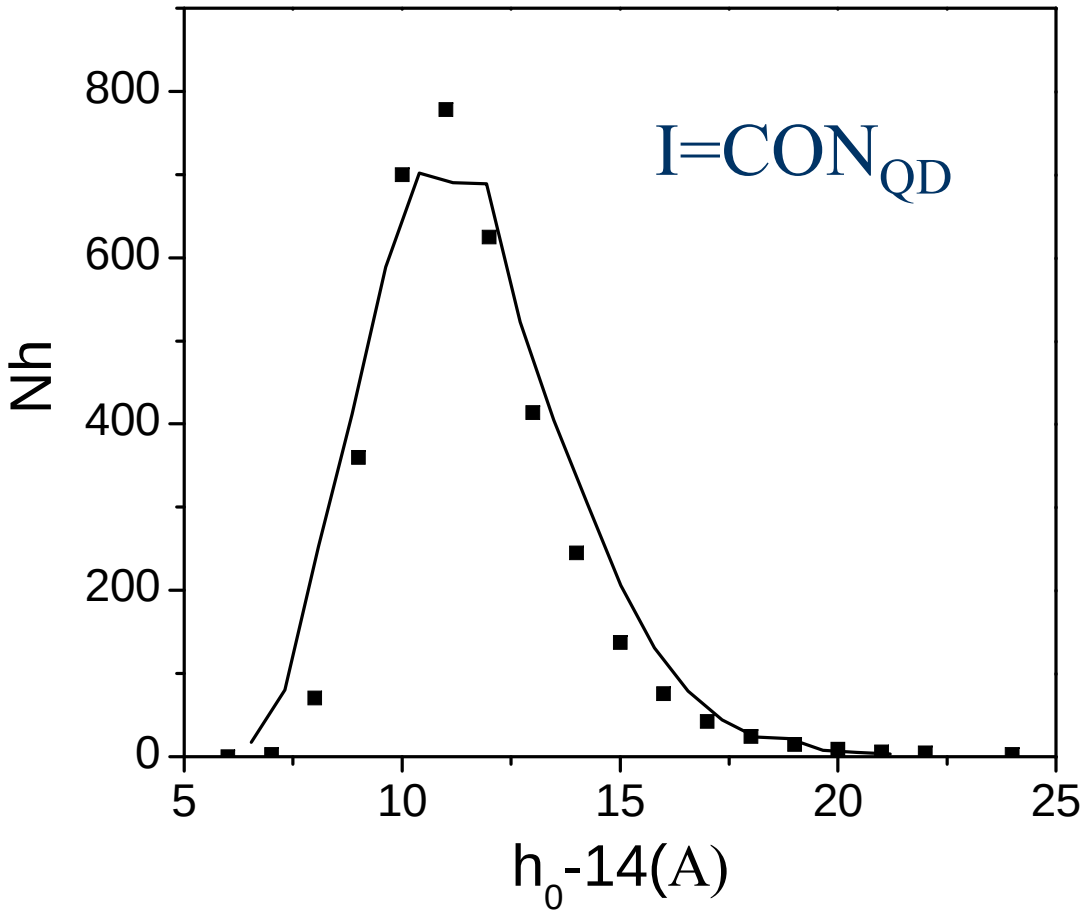

Solid curve: AFM measurement N_{QD}

Dots: theoretical calculations

C is an arbitrary constant.

O is the overlap integral.

Temperature dependent PL

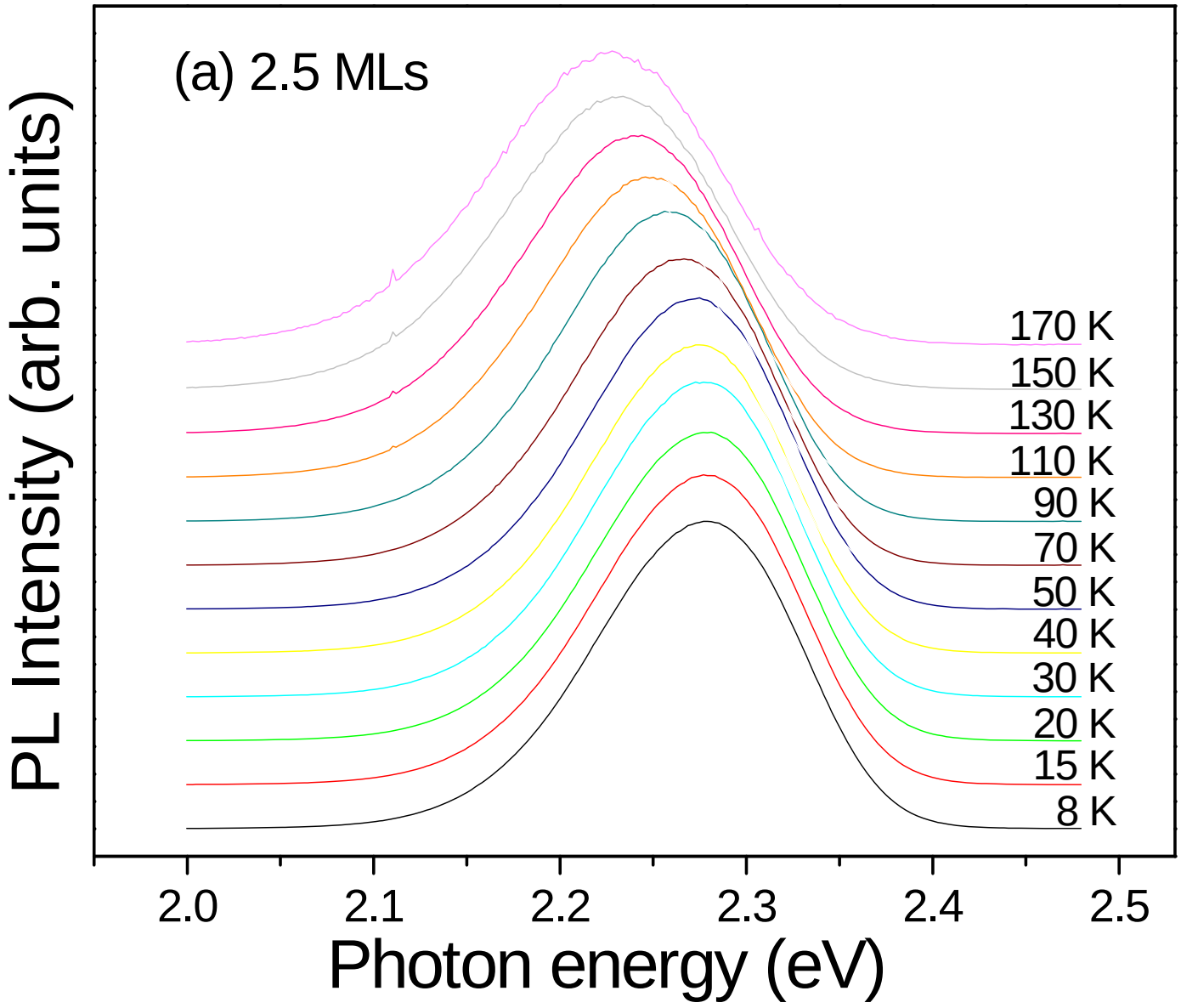

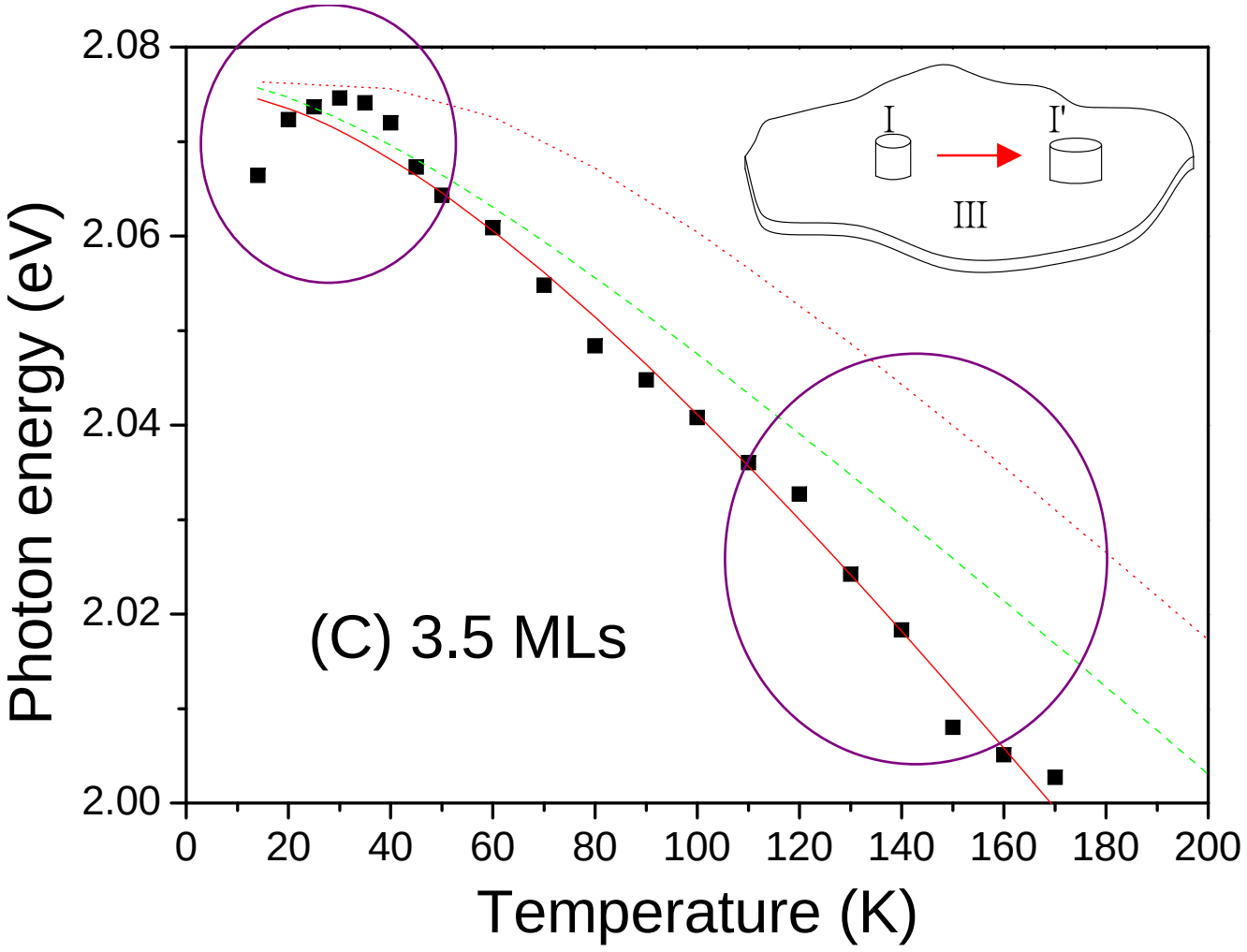

Signature of carrier transfer between smaller dot - wetting layer - larger dot. Initial blue shift at low T, then a fast red shift. The red-shift is about 0.5 meV/K for QD and is much larger than that of ZnTe epilayer of roughly 0.35 meV/K.

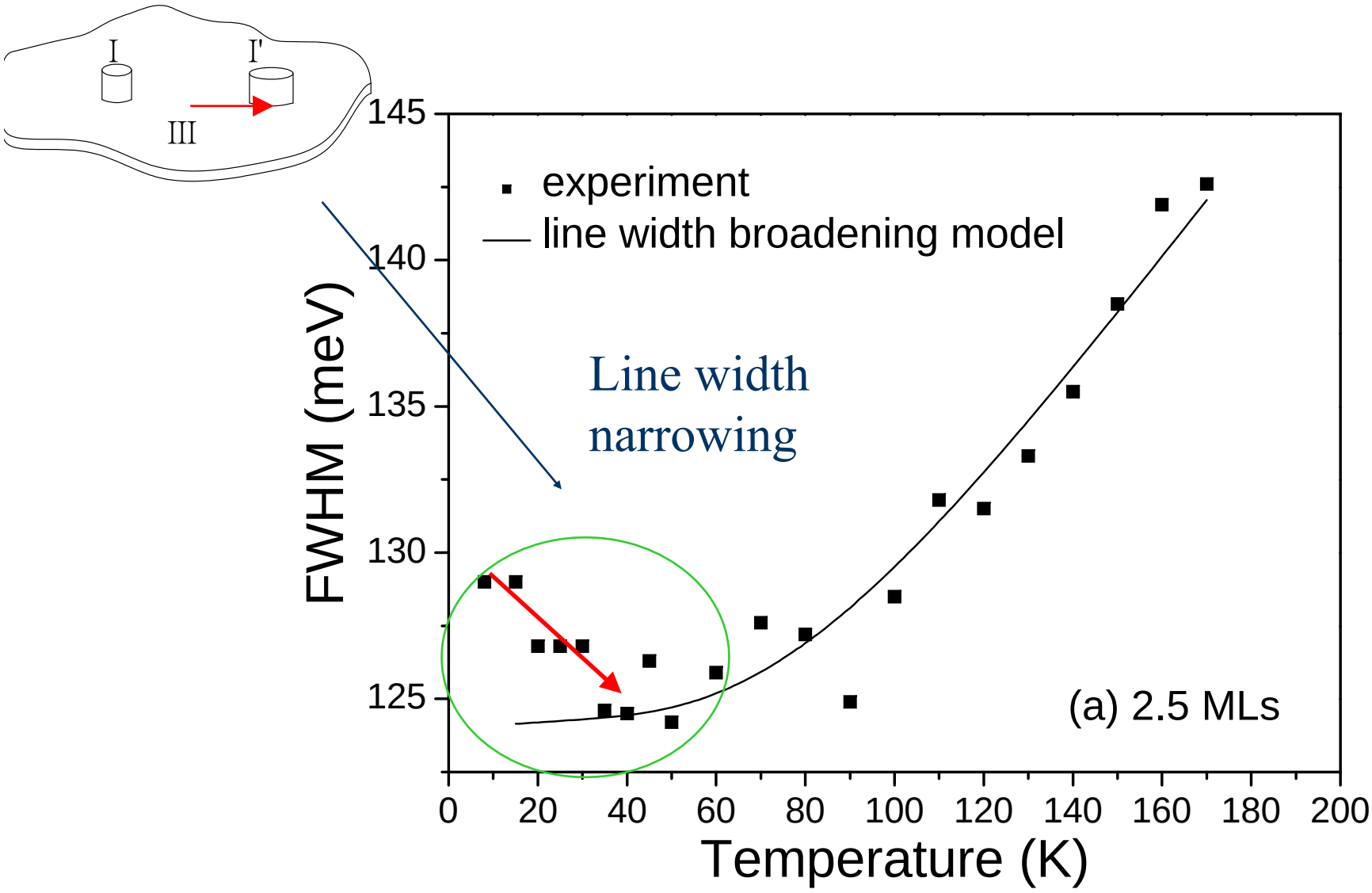

Solid curve is obtained by the fit:

$$\Gamma(T) = \Gamma_0 + \Gamma_a T + \Gamma_{LO} / [\exp(\hbar\omega_{LO} / kT) - 1] + \Gamma_i \exp(-\langle E_b \rangle / kT)$$

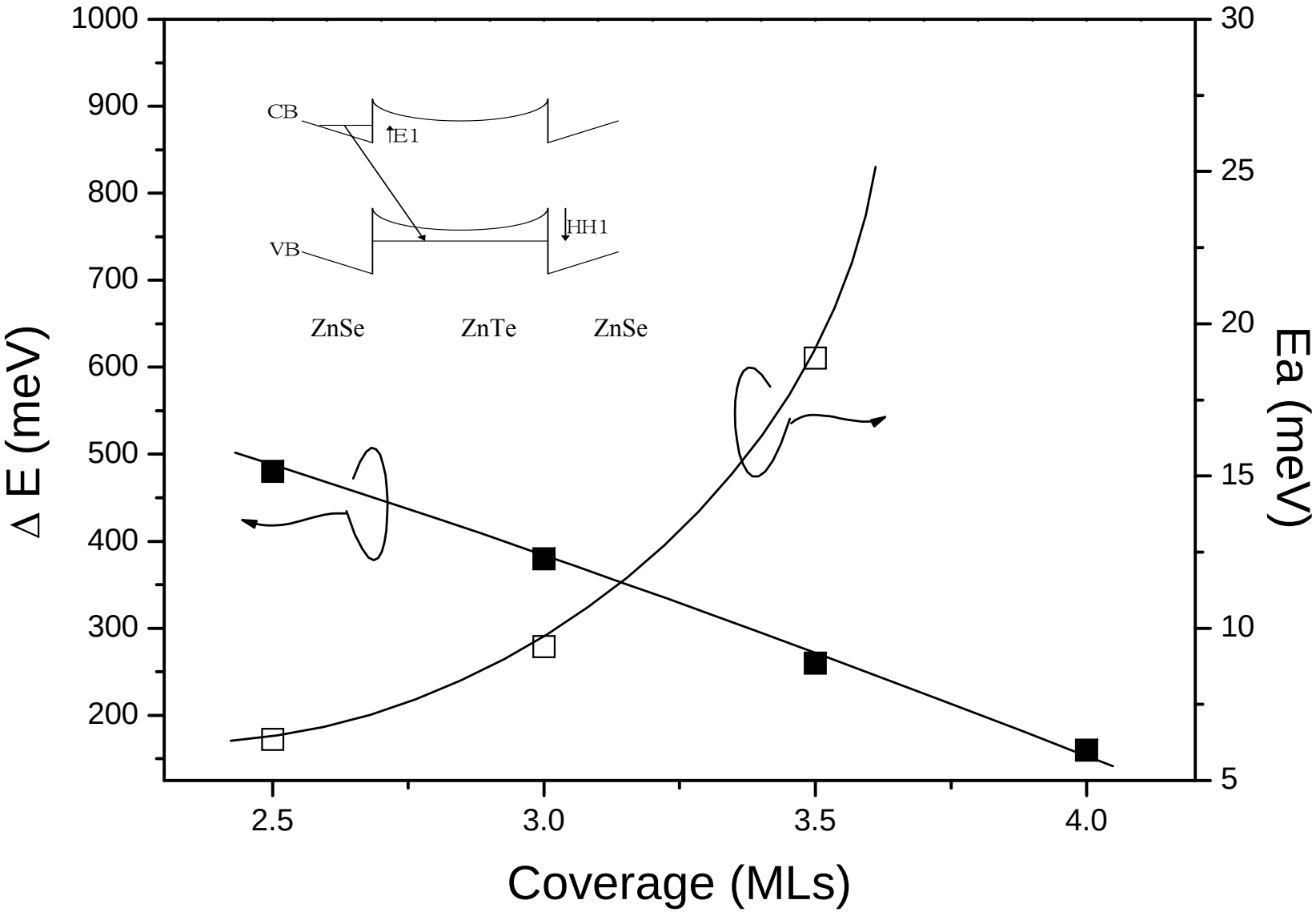

The energy difference (Δ E) and activation energy (Ea) were plotted versus the ZnTe coverage. A bended band structure was schematically drawn in the insert.

Single-electron charging of a self-assembled II–VI quantum dot

J. Seufert,[a)] M. Rambach, G. Bacher, and A. Forchel
Technische Physik, Universität Würzburg, Am Hubland, D-97074 Würzburg, Germany

T. Passow and D. Hommel
Institut für Festkörperphysik, Universität Bremen, D-28359 Bremen, Germany

APL v82, 3946 (2004)

We have studied single-electron injection into individual self-assembled CdSe/ZnSe quantum dots. Using nanostructured contacts to apply a vertical electric field, excess electrons are promoted to the single-quantum-dot ground state in a controlled fashion. Spatially-resolved photoluminescence spectroscopy is applied to demonstrate single-quantum-dot charging via the formation of single zero-dimensional charged excitons with a binding energy on the order of 10 meV. [DOI: 10.1063/1.1580632]

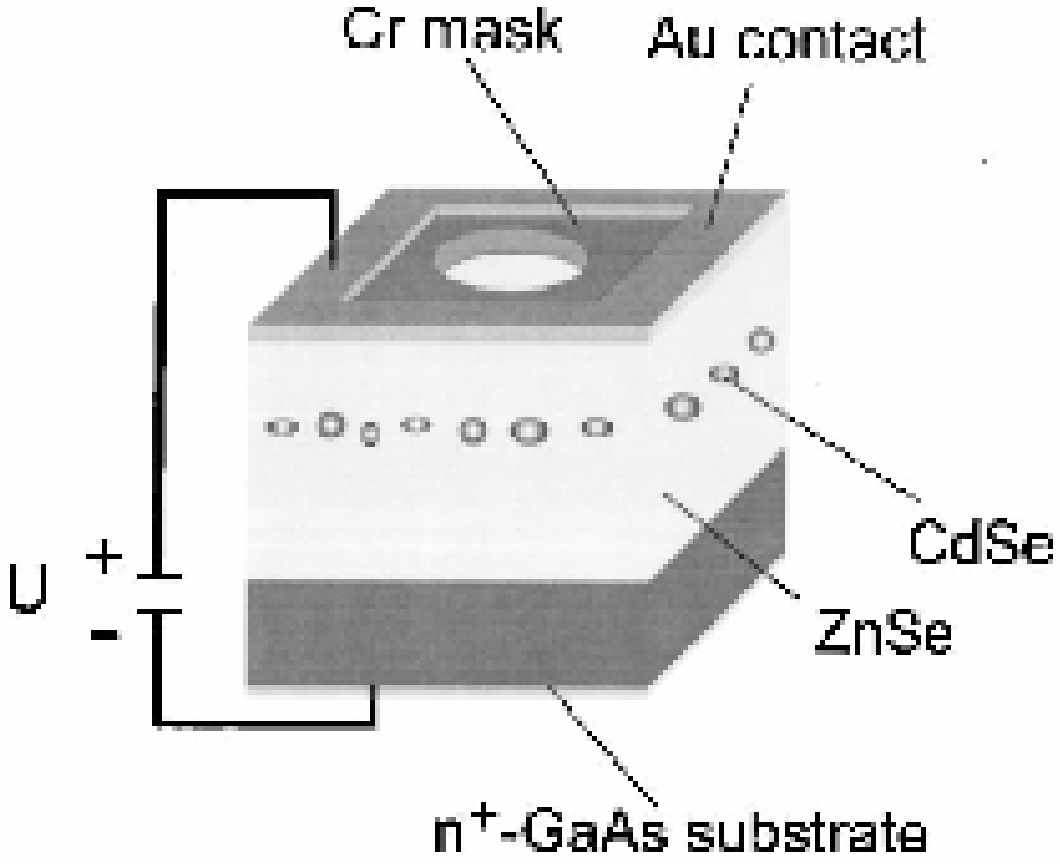

FIG. 1. Schematic representation of the sample design for the spectroscopy of single quantum dots in a vertical electric field.

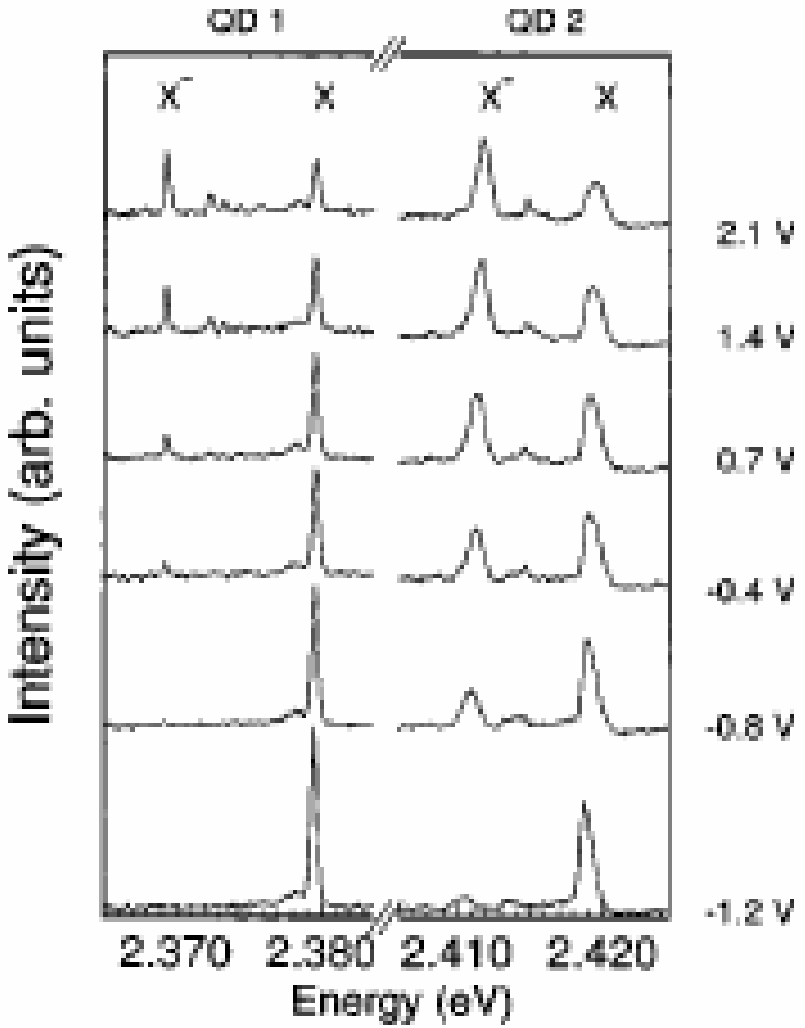

FIG. 2. PL spectra of two individual QDs (QD1 and QD2) obtained using a nanoaperture of diameter 200 nm for various values of an applied bias voltage. Single luminescence lines labeled as X (X^-) correspond to the emission from the neutral (charged) exciton transition.

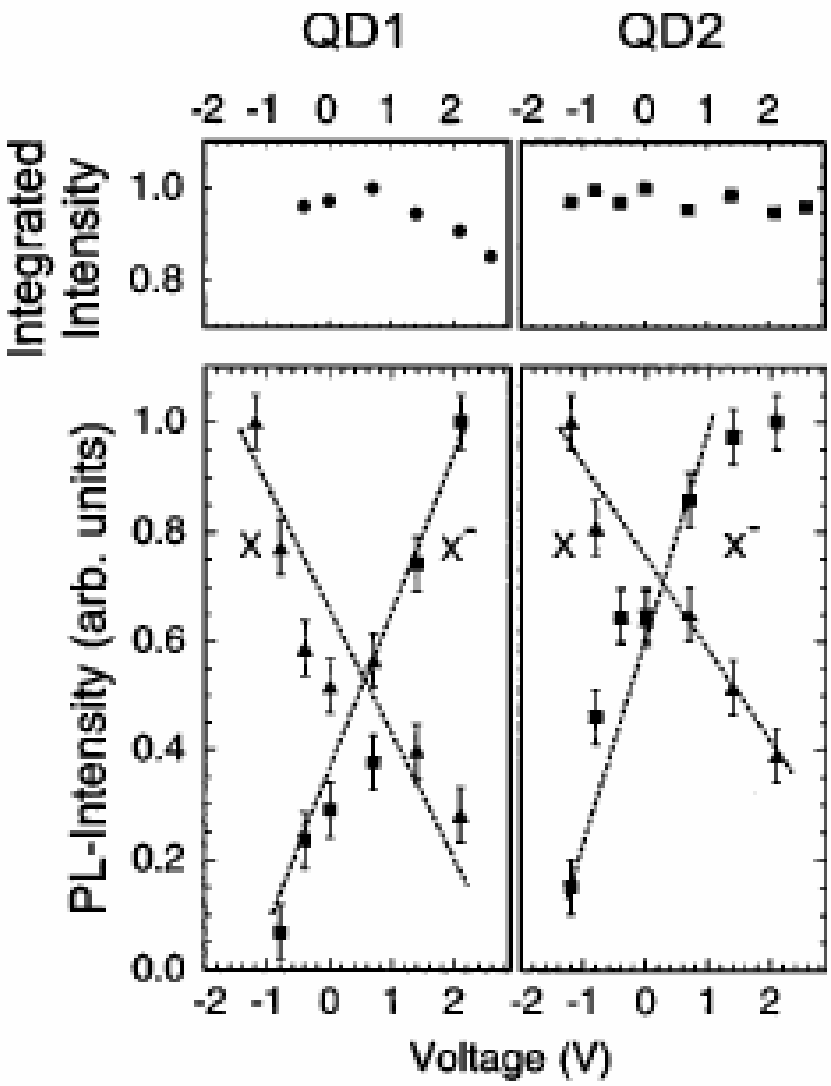

FIG. 3. Bottom: PL intensities of the neutral and the charged exciton transition in two single QDs as a function of the applied voltage. Top: Summarized intensity of the neutral and charged exciton transition for each QD.

Near-Field Optical Mapping of Exciton Wave Functions in a GaAs Quantum Dot

K. Matsuda,[1,2,*] T. Saiki,[1,3] S. Nomura,[4,5] M. Mihara,[5] Y. Aoyagi,[5,6] S. Nair,[7] and T. Takagahara[8]

PRL v91, 177401 (2003)

Near-field photoluminescence imaging spectroscopy of naturally occurring GaAs quantum dots (QDs) is presented. We successfully mapped out center-of -mass wave functions of an exciton confined in a GaAs QD in real space due to the enhancement of spatial resolution up to 30 nm. As a consequence, we discovered that the spatial profile of the exciton emission, which reflects the shape of a monolayer-high island, differs from that of biexciton emission, due to different distributions of the polarization field for the exciton and biexciton recombinations. This novel technique can be extensively applied to wave function engineering in the design and the fabrication of quantum devices.

Theoretical studies predict that the optical LDOS is directly connected to the (center-of-mass) wave functions of electron-hole pair (exciton) via the calculation of transition rate as a function of probe position [17,18]. Such a possibility, however, has not been investigated while NSOM contribute to the spectroscopy of a single quantum object by isolating individual components with a spatial resolution of 100–200 nm [19–22]. Enhancement of spatial resolution up to 10–30 nm, which is smaller than the typical size of quantum constituents, is of critical importance to precisely map out the wave function of a confined exciton.

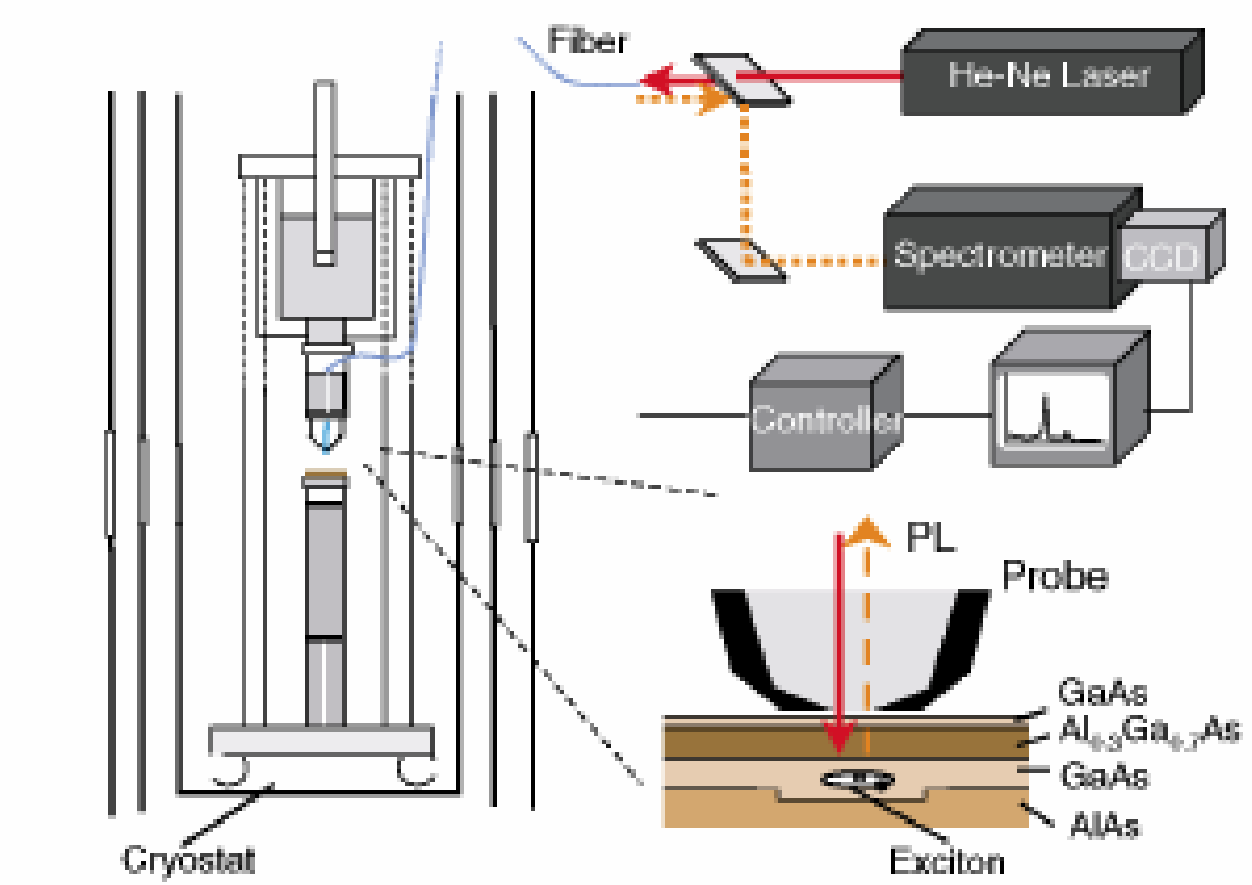

FIG. 1 (color). Schematic of low temperature near-field scanning optical microscope and experimental setup of near-field photoluminescence (PL) measurement. Sample structures of naturally occurring quantum dot (QD) in a narrow quantum well and the near-field probe are shown.

The critical element in the high-resolution NSOM measurement was an optical fiber probe, which was fabricated by chemical etching with a hydrofluoric acid solution [22,23]. The tapered structure was optimized by taking account of trade-off between optical throughput and spatial resolution. A small clear aperture was prepared by pounding the probe apex against the sample surface under shear-force feedback control. The aperture diameter (20 nm) was estimated from scanning electron micrographs, taken after conducting near-field imaging measurements at cryogenic temperature. A spatial resolution as high as 30 nm was demonstrated by low temperature PL imaging of self-assembled InAs QDs with a 30 nm aperture probe [23]. The sample of GaAs QDs was excited with He-Ne laser light ($\lambda = 633$ nm) through the aperture and the resultant PL signal was collected via the same aperture to prevent a reduction of the spatial resolution due to carrier diffusion as shown in Fig. 1 [24]. Near-field PL spectra were measured, for example, at 11 nm steps across a 210×210 nm^2 area and two-dimensional images were constructed from a series of PL spectra.

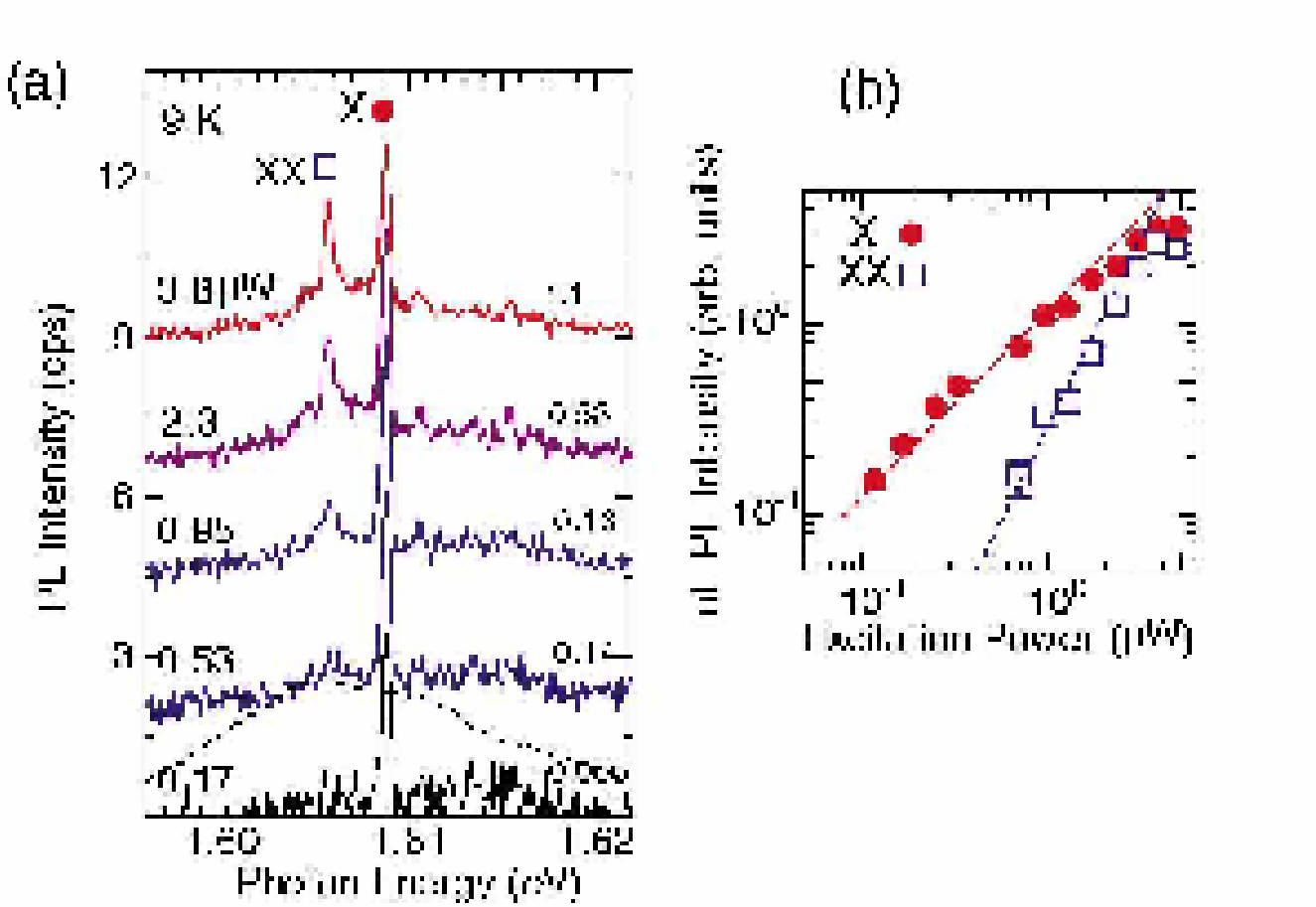

FIG. 2 (color). Near-field PL spectra of a single QD (solid lines) and far-field PL spectrum (dotted line) at 9 K (a). The PL peaks at 1.6088 and 1.6057 eV are denoted by X and XX. Excitation power dependence of integrated PL intensities of the X and the XX lines (b). The red (blue) dotted line corresponds to the gradient associated with linear (quadratic) power dependence. Near-field PL images obtained by mapping the intensity of the X lines in a same scanning area (1000× 1000 nm^2) (c)–(e). The PL spectra for generating each image are indicated (f). The QDs in (c) and (d) are in one-monolayer

Excitation power dependence of integrated PL intensities of the X and the XX lines (b). The red (blue) dotted line corresponds to the gradient associated with linear (quadratic) power dependence. Near-field PL images obtained by mapping the intensity of the X lines in a same scanning area (1000× 1000 nm^2) (c)–(e). The PL spectra for generating each image are indicated (f). The QDs in (c) and (d) are in one-monolayer thinner regions and the one in (e) is in a one-monolayer thicker region.

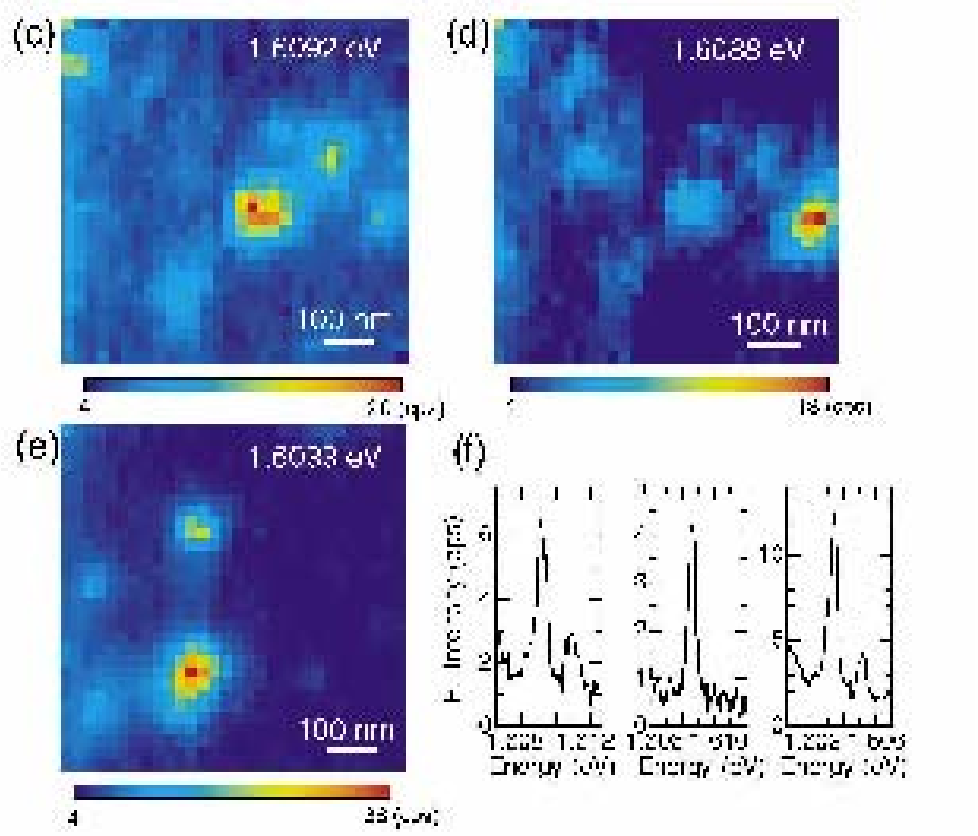

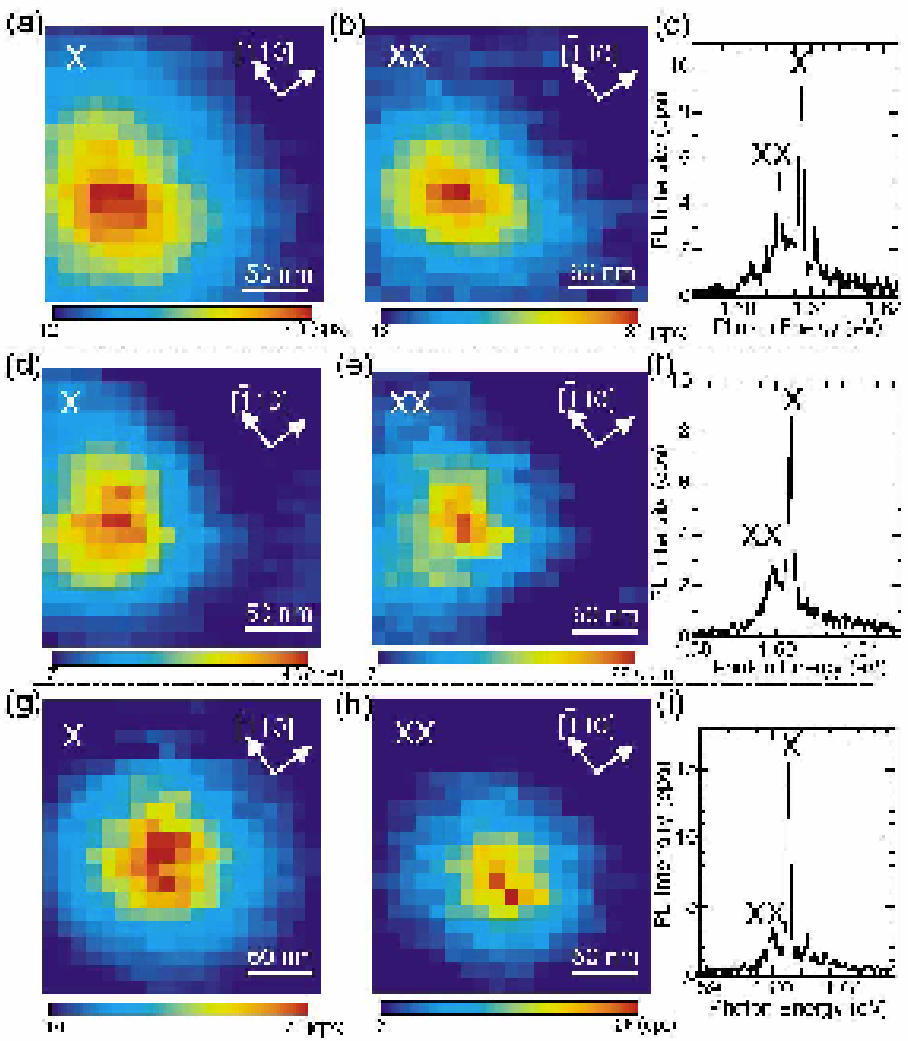

FIG. 3 (color). (a)–(i) Series of high-resolution PL images of exciton state [(a), (d), and (g)], biexciton state [(b), (e), and (h)], and corresponding PL spectra [(c), (f), and (i)] for three different QDs. Scanning area is 210×210 nm^2. Crystal axes along [110] and [$\bar{1}$10] directions are indicated. PL image sizes of biexciton are always smaller than those of exciton.